Energy Conversion and Management 80 (2014) 243–255

Contents lists available at ScienceDirect

Energy Conversion and Management

journal homepage: www.elsevier.com/locate/enconman

Performance analysis of waste heat recovery with a dual loop organic Rankine cycle (ORC) system for diesel engine under various operating conditions

Fubin Yang [a], Xiaorui Dong [a], Hongguang Zhang [b,*], Zhen Wang [a], Kai Yang [b], Jian Zhang [b], Enhua Wang [b], Hao Liu [b], Guangyao Zhao [b]

[a] School of Mechanical and Power Engineering, North University of China, Xueyuan Road No. 3, 030051 Taiyuan, China
[b] College of Environmental and Energy Engineering, Beijing University of Technology, Pingleyuan No. 100, 100124 Beijing, China

ARTICLE INFO

Article history:
Received 12 July 2013
Accepted 20 January 2014
Available online 13 February 2014

Keywords:
Dual loop organic Rankine cycle
Diesel engine
Waste heat recovery
Various operating conditions
Performance analysis

ABSTRACT

To take full advantage of the waste heat from a diesel engine, a set of dual loop organic Rankine cycle (ORC) system is designed to recover exhaust energy, waste heat from the coolant system, and released heat from turbocharged air in the intercooler of a six-cylinder diesel engine. The dual loop ORC system consists of a high temperature loop ORC system and a low temperature loop ORC system. R245fa is selected as the working fluid for both loops. Through the engine test, based on the first and second laws of thermodynamics, the performance of the dual loop ORC system for waste heat recovery is discussed based on the analysis of its waste heat characteristics under engine various operating conditions. Subsequently, the diesel engine-dual loop ORC combined system is presented, and the effective thermal efficiency and the brake specific fuel consumption (BSFC) are chosen to evaluate the operating performances of the diesel engine-dual loop ORC combined system. The results show that, the maximum waste heat recovery efficiency (WHRE) of the dual loop ORC system can reach 5.4% under engine various operating conditions. At the engine rated condition, the dual loop ORC system achieves the largest net power output at 27.85 kW. Compared with the diesel engine, the thermal efficiency of the combined system can be increased by 13%. When the diesel engine is operating at the high load region, the BSFC can be reduced by a maximum 4%.

1. Introduction

With the rapid development of the auto industry, the automobile population has skyrocketed, and the energy sources consumed by automobiles have been growing rapidly. Meanwhile, given the low utilization rate, the effective power output of the total fuel combustion energy is less than 40% in internal combustion (IC) engines, and the remaining heat is released into the atmosphere. This mechanism not only harms the environment; it also results in energy dissipation. Currently, numerous research institutes and scholars are devoted to developing new energy vehicles and alternative fuel technologies. Therein, biodiesel is a kind of clean biofuel that holds much promise. However, the application of biodiesel remains limited by technology and cost, such that this technology cannot displace traditional IC engines in the near future [1–3]. Therefore, recovering the waste heat from IC engines is an effective method for the improvement of thermal efficiency, reducing pollutant emission, and saving fuel.

Reasonable measures should be employed to recover and utilize the low-grade waste heat of IC engines. Numerous scholars have recently investigated the use of organic Rankine cycle (ORC) system to recover low-grade waste heat. Research has focused on the selection of working fluids, optimization parameters, system configuration improvements, and so on. Mago et al. employed a basic ORC system and a regenerative ORC system to convert waste energy into power from low-grade heat sources. The results showed that the regenerative ORC system achieved a higher efficiency compared with the basic ORC system [4]. Wang et al. presented a method for selecting the working fluid and parametric optimization using a multi-objective optimization model by simulated annealing algorithm. They concluded that different working fluids should be selected to match the different heat source temperatures [5]. Roy et al. designed a set of ORC system, using R-12, R-123 and R134a as working fluids to recover the waste heat from flue gas. The analysis showed that R-123 had the maximum

* Corresponding author. Tel.: +86 10 6739 2469; fax: +86 10 6739 2774.
E-mail address: zhanghongguang@bjut.edu.cn (H. Zhang).

http://dx.doi.org/10.1016/j.enconman.2014.01.036
0196-8904/

Nomenclature

$\dot{W}$	power (kW)
$\dot{Q}$	heat transfer rate (kW)
$\dot{m}$	mass flow rate (kg/s)
h	specific enthalpy (kJ/kg)
s	specific entropy (kJ/kg K)
$\dot{I}$	exergy destruction rate (kW)
T	temperature (K)
P	pressure (MPa)
$\dot{F}$	fuel consumption (kg/h)
x, y, z	mole amount
bsfc	brake specific fuel consumption (g/kW h)

Greek letters

η	efficiency
ε	effectiveness of the recuperator
φ	heat transfer efficiency
χ	mass fraction

Subscript

0	reference state
H	high temperature loop ORC system
L	low temperature loop ORC system
H1, H2, H2s, H3, H4, H5, H5s, H6	state points in HT loop ORC system
L1, L2, L2s, L3, L4, L4s, L5, L6	state points in LT loop ORC system
p1	pump 1
p2	pump 2
r	recuperator
e1	evaporator 1
e2	evaporator 2
exp1	expander 1
exp2	expander 2
pre	preheater
int	intercooler
a	intake air
in	at the inlet
out	at the outlet
con	condenser
n	net
oa	overall
w	waste
exh	exhaust gas
cool	coolant
HTH	high temperature heat source in HT loop ORC system
HTL	high temperature heat source in LT loop ORC system
LTL	low temperature heat source in LT loop ORC system
HS	heat source
comb	combustion
f	fuel
misc	miscellaneous
th	thermal
eff	effective
cs	combined system
eng	engine

Acronyms

ORC	organic Rankine cycle
HT	high temperature
LT	low temperature
WHRE	waste heat recovery efficiency
BSFC	brake specific fuel consumption
ODP	ozone depletion potential (relative to R11)
GWP	global warming potential (relative to CO_2)
IC	internal combustion

work output and efficiencies among all the selected fluids [6]. Wei et al. studied the performance and optimization of an ORC system using HFC-245fa (1,1,1,3,3-penta-fluoropropane) as a working fluid driven by exhaust heat. The results revealed that utilizing the exhaust heat as much as possible was a good method for improving the system output net power and efficiency [7]. Liu et al. presented a two stage Rankine cycle for power generation, which was composed of a water steam Rankine cycle and an Organic Rankine bottoming cycle. Optimal points were found at different cold source temperatures and steam turbine outlet pressures for each cycle [8]. Wang et al. conducted a multi-objective optimization of the ORC system to achieve the system optimization design from both thermodynamic and economic aspects using an evolutionary algorithm [9]. Gao et al. assessed 18 organic working fluids according to their physical and chemical properties for a supercritical ORC driven by exhaust heat. The effects of these working fluids on the performance of the supercritical ORC system were discussed. The results showed that R152a and R143a are recommended as the working fluids for the supercritical ORC system [10]. Hung proposed an ORC system to recover waste heat from low enthalpy heat sources using dry fluids. The study indicated that R113 and R123 performed better in recovering low temperature waste heat [11]. Quoilin et al. proposed a dynamic ORC model and three different control strategies. Their simulation results showed that a model predictive control strategy based on the steady-state optimization of the cycle under various conditions was the one showed the best results [12]. Dai et al. described an ORC for recovering low-grade waste heat using different working fluids. The effects of thermodynamic parameters on ORC performance were examined, and the thermodynamic parameters of the ORC for each working fluid were optimized with exergy efficiency as an objective function. The results indicated that the cycle with R236EA had the highest exergy efficiency [13]. Guo et al. proposed an innovative cogeneration system powered by low temperature geothermal sources, and the system consisted of a low temperature geothermal-powered ORC subsystem, an intermediate heat exchanger, and a commercial R134a-based heat pump subsystem. The suitable working fluids were screened and the performances of the novel cogeneration system under disturbance conditions were studied [14]. Hung et al. investigated the effects of dry, wet, and isentropic organic fluids as working fluids on the performance of ORC system. The results revealed that wet organic fluids with very steep saturated vapor curves in T–s diagram had a better overall performance in terms of energy conversion efficiencies than that of dry organic fluids. Furthermore, an appropriate combination of solar energy and an ORC system with a higher turbine inlet temperature and a lower condenser temperature would provide an economically feasible energy conversion system [15]. Wang et al. conducted an experimental study to investigate the performance of a low temperature solar Rankine cycle system. The results showed that the highest heat collecting efficiency of the collector is about 50% [16].

The ORC system has been widely applied to the recovery of waste heat from IC engines. Gao et al. proposed a waste heat recovery system where a high-speed turbocharged diesel engine acts as the topper of a combined cycle system and exhaust gases were used for a bottoming Rankine cycle. The conclusion was that introducing a heat recovery system could increase the engine power output by 12% [17]. Srinivasan et al. designed an ORC system to

examine the exhaust waste heat recovery potential of a high-efficiency, low-emissions dual fuel low temperature combustion engine [18]. Vaja et al. considered three different ORC setups for recovering the waste heat of exhaust gases and engine cooling water. The analysis demonstrated that a 12% increase in the overall efficiency could be achieved with respect to the engine with no bottoming [19]. Yu et al. built an ORC system to recover waste heat both from engine exhaust gas and jacket water using R245fa as working fluid. The results indicated that the ORC system performs well under the rated engine condition with a recovery efficiency of up to 9.2% and exergy efficiency of up to 21.7% [20]. Tian et al. proposed an ORC system used in the IC engine exhaust heat recovery and techno-economical performances of the ORC system based on various working fluids. The results showed that R141b, R123, and R245fa had the highest thermal efficiency and the lowest electricity production cost [21]. Katsanos et al. investigated the potential improvement in the overall efficiency of a heavy-duty truck diesel engine equipped with a Rankine bottoming cycle for recovering heat from exhaust gas. They discovered that the specific fuel consumption improvement ranged from 10.2% (at 25% engine load) to 8.5% (at 100% engine load) for R245ca [22]. Wang et al. analyzed the characteristics of a novel system combining a gasoline engine with a dual loop ORC system that recovered the waste heat from both the exhaust and coolant system [23]. Peng et al. developed an Exhaust Energy Recovery (EER) system based on Rankine cycle to convert exhaust thermal energy to mechanical or electric energy [24]. Wang et al. investigated the improvement on a light-duty gasoline engine with experimental work and a numerical simulation based on a steam Rankine cycle EER system [25].

From the aforementioned analysis, ORC system is efficient for recovering the waste heat from IC engines. Currently, however, most research takes only IC engine exhaust energy into account. Few scholars have considered recovering the waste heat from the coolant system, and the released heat from turbocharged air in the intercooler of IC engine. In this paper, a set of dual loop ORC system is designed to recover exhaust energy, waste heat from the coolant system, and released heat from turbocharged air in the intercooler of a six-cylinder diesel engine. The dual loop ORC system consists of a high temperature (HT) loop ORC system and a low temperature (LT) loop ORC system. R245fa was selected as the working fluid for both loops. The HT loop ORC system is used to recover the exhaust energy, whereas the LT loop ORC system is used to recover the waste heat from the coolant system, the released heat from turbocharged air in the intercooler, and the released heat from the condensation process of the HT loop ORC system. First, the distribution characteristics of the waste heat from the diesel engine under various operating conditions are analyzed via a diesel engine performance test. Thereafter, the operating performances of the dual loop ORC system and the diesel engine-dual loop ORC combined system are evaluated.

2. Dual loop ORC system

2.1. System description

Exhaust temperature is generally high when the diesel engine is running. However, the temperature of the coolant and the turbocharged air in the intercooler is relatively low. To take full advantage of the waste heat from the diesel engine, a set of dual loop ORC system is designed for a six-cylinder diesel engine. As shown in Fig. 1, the dual loop ORC system contains a HT loop ORC system (the red[1] lines in Fig. 1) and a LT loop ORC system (the purple lines in Fig. 1). The HT loop ORC system is used to recover the exhaust energy, while the LT loop ORC system is used to recover the waste heat from the coolant system, the released heat from turbocharged air in the intercooler, and the released heat from the condensation process of the HT loop ORC system. The HT loop ORC system consists of an evaporator (Evaporator 1), an expander (Expander 1), a generator (Generator 1), a recuperator, a preheater, and a pump (Pump 1). The LT loop ORC system consists of an evaporator (Evaporator 2), an expander (Expander 2), a generator (Generator 2), a condenser, a pump (Pump 2), an intercooler, and a preheater. The two separate ORC systems are coupled using the preheater.

The selected working fluid plays an important role in the thermodynamic performances of the dual loop ORC system. The environmental impact and safety level of the working fluid should be considered, and the selected working fluid should make the system more efficient and stable; R245fa can meet these demands well [26]. Therefore, R245fa is selected as the working fluid for this study. The thermodynamic properties are evaluated using REFPROP 8.0 [27], which was developed by the National Institute of Standards and Technology in the United States. The properties of R245fa are listed in Table 1.

The working principle of the dual loop ORC system is illustrated in Fig. 1. In the HT loop ORC system, the working fluid is pressurized into a subcooled liquid state using Pump 1. Then it is preheated in the recuperator. Subsequently, the working fluid is sent to Evaporator 1 and turns into a saturated vapor state. Then, the saturated vapor enters Expander 1 to produce useful work and the useful work is used to generate electricity. Finally, the superheated vapor exported from Expander 1 turns into a saturated liquid state after the heat transfer process in the recuperator and preheater. With this change, the HT loop ORC system completes one working cycle. Meanwhile, in the LT loop ORC system, the working fluid is pressurized using Pump 2 and becomes a subcooled liquid state. Then, the working fluid is sent into the intercooler to exchange heat with the turbocharged intake air. After this, the working fluid flows into the preheater and is heated up into the two-phase state by the released heat during the condensation process of the HT loop ORC system. Later, the two-phase working fluid is heated up into a saturated vapor state by the engine coolant in the Evaporator 2. The saturated vapor enters Expander 2 to make it do work and make Generator 2 produce electricity. Finally, the superheated vapor exported from Expander 2 condenses into a saturated liquid state in the condenser. The whole process is then completed.

2.2. Thermodynamic model

The thermodynamic model of the dual loop ORC system is developed based on the first and second laws of thermodynamics. The *T–s* diagram of the dual loop ORC system is shown in Fig. 2. The red lines represent the HT loop ORC, whereas the purple lines corresponded to the LT loop ORC.

2.2.1. HT loop ORC process

Pump phase (stages H4–H5):

The power consumed by Pump 1 and its exergy destruction rate are calculated using the following equations:

$$\dot{W}_{p1} = \dot{m}_H(h_{H5} - h_{H4}) \tag{1}$$

$$\dot{I}_{p1} = T_0\dot{m}_H(s_{H5} - s_{H4}) \tag{2}$$

The isentropic efficiency of Pump 1 is given by:

$$\eta_{p1} = \frac{h_{H5s} - h_{H4}}{h_{H5} - h_{H4}} \tag{3}$$

Recuperator phase (stages H5–H6, H2–H3):

[1] For interpretation of color in Fig. 1, the reader is referred to the web version of this article.

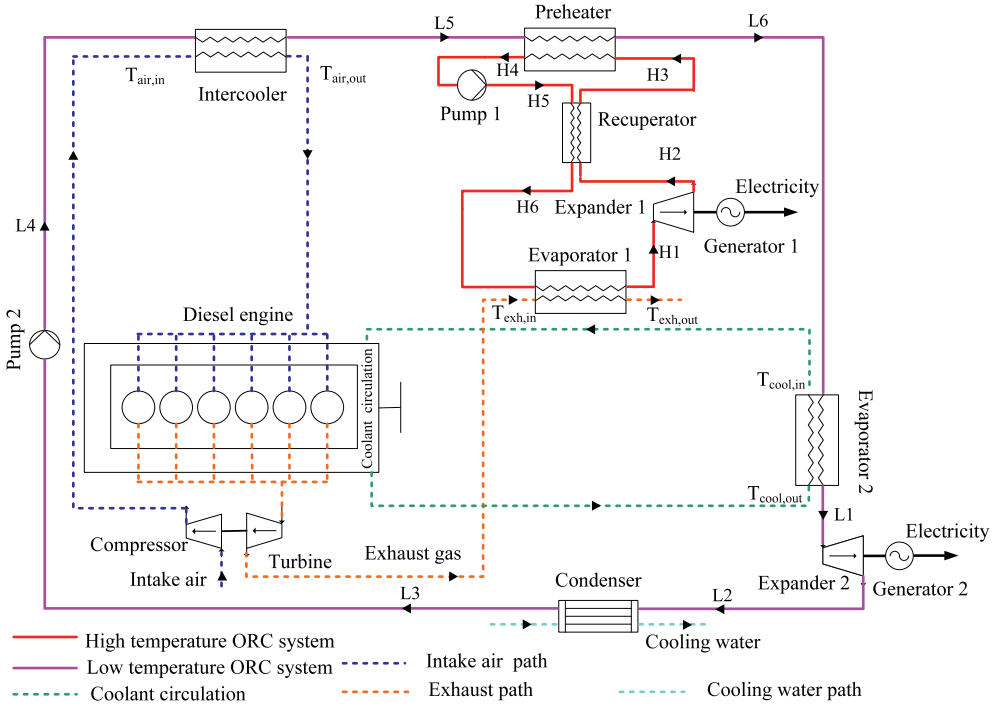

Fig. 1. Schematic diagram of the dual loop ORC system.

Table 1
Properties of R245fa.

Parameters	Values
Molecular formula	$CHF_2CH_2CF_3$
Molecular weight (kg/kmol)	134.05
Critical temperature (K)	427.16
Critical pressure (MPa)	3.65
Boiling temperature (K)	288.29
ASHRAE 34 safety group	B1
Atmospheric life time (yr)	7.2
ODP	0
GWP (100 yr)	950

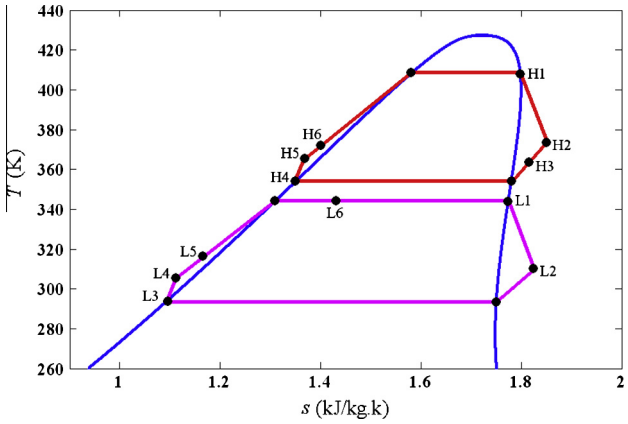

Fig. 2. *T*–*s* diagram of the dual loop ORC system.

The effectiveness of the recuperator can be determined as [22]:

$$\varepsilon = \frac{T_{H2} - T_{H3}}{T_{H2} - T_{H5}} \tag{4}$$

The heat transfer rate of the recuperator and its exergy destruction rate are respectively calculated using the following equations:

$$\dot{Q}_r = \dot{m}_H(h_{H2} - h_{H3}) = \dot{m}_H(h_{H6} - h_{H5}) \tag{5}$$

$$\dot{I}_r = \dot{T}_0\dot{m}_H[(s_{H3} - s_{H2}) + (s_{H6} - s_{H5})] \tag{6}$$

Evaporator phase (stages H6–H1):

The heat transfer rate of Evaporator 1 and its exergy destruction rate are calculated using the equations below respectively [26]:

$$\dot{Q}_{e1} = \dot{m}_{exh}(h_{exh,in} - h_{exh,out}) = \dot{m}_H(h_{H1} - h_{H6}) \tag{7}$$

$$\dot{I}_{e1} = T_0\dot{m}_H\left[(s_{H1} - s_{H6}) - \frac{h_{H1} - h_{H6}}{T_{HTH}}\right] \tag{8}$$

When the exhaust temperature drops below the dew point, the exhaust pipes and evaporator surfaces can erode [28]. Therefore, in this study, the exhaust temperature at the outlet of the Evaporator 1 is set to 378.15 K. The exhaust temperature and pressure at the inlet of Evaporator 1 can be measured through the engine test bench, such that the enthalpy of the exhaust can be computed. Using Eq. (7), the heat transfer rate of Evaporator 1 can be calculated. In Eq. (7), T_{HTH} is the temperature of the high temperature heat source in the HT loop ORC system. For, exhaust gas as high temperature heat source, the temperature of the exhaust gas is changing during the process. This temperature is assumed to be equal to $T_{HTH} = T_{H1} + 5$ [29].

Expander phase (stages H1–H2):

The power output of the Expander 1 and its exergy destruction rate are calculated using the equations below respectively:

$$\dot{W}_{exp1} = \dot{m}_H(h_{H1} - h_{H2}) \tag{9}$$

$$\dot{I}_{exp1} = T_0\dot{m}_H(s_{H2} - s_{H1}) \tag{10}$$

The isentropic efficiency of the Expander 1 is given by:

$$\eta_{exp1} = \frac{h_{H1} - h_{H2}}{h_{H1} - h_{H2s}} \tag{11}$$

Preheater phase (stages H3–H4):

The heat transfer rate in the preheater is calculated as:

$$\dot{Q}_{H,pre} = \dot{m}_H(h_{H3} - h_{H4}) \tag{12}$$

2.2.2. LT loop ORC process

Pump phase (stages L3–L4):

The power consumed by Pump 2 and its exergy destruction rate are respectively calculated using the following equations:

$$\dot{W}_{p2} = \dot{m}_L(h_{L4} - h_{L3}) \tag{13}$$

$$\dot{I}_{p2} = T_0\dot{m}_L(s_{L4} - s_{L3}) \tag{14}$$

The isentropic efficiency of the Pump 2 is given by:

$$\eta_{p2} = \frac{h_{L4s} - h_{L3}}{h_{L4} - h_{L3}} \tag{15}$$

Intercooler phase (stages L4–L5):

The heat transfer rate of the intercooler and its exergy destruction rate are respectively calculated using the following equations:

$$\dot{Q}_{int} = \dot{m}_L(h_{L5} - h_{L4}) = \dot{m}_{air}(h_{air,in} - h_{air,out}) \tag{16}$$

$$\dot{I}_{int} = T_0\dot{m}_L\left[(s_{L5} - s_{L4}) - \frac{h_{L5} - h_{L4}}{T_{int,HS}}\right] \tag{17}$$

where $T_{int,HS}$ is the temperature of the heat source in the intercooler. This temperature is assumed to be equal to$T_{int,HS} = T_{L5} + 5$.

Preheater phase (stages L5–L6):

The heat transfer rate of preheater and its exergy destruction rate are respectively calculated using the following equations:

$$\dot{Q}_{L,pre} = \dot{m}_L(h_{L6} - h_{L5}) = \varphi_{pre}\dot{Q}_{H,pre} \tag{18}$$

$$\dot{I}_{pre} = T_0\dot{m}_H(s_{H4} - s_{H3}) + T_0\dot{m}_L(s_{L6} - s_{L5}) \tag{19}$$

where φ_{pre} is the heat transfer efficiency of the preheater.

Evaporator phase (stages L6–L1):

The heat transfer rate of the evaporator 2 and its exergy destruction rate are respectively calculated using the following equations:

$$\dot{Q}_{e2} = \dot{m}_L(h_{L1} - h_{L6}) = \varphi_{cool}\dot{Q}_{cool} \tag{20}$$

$$\dot{I}_{e2} = T_0\dot{m}_L\left[(s_{L1} - s_{L6}) - \frac{h_{L1} - h_{L6}}{T_{HTL}}\right] \tag{21}$$

where $\dot{Q}_{cool}$ is the waste heat quantity carried by the engine coolant system and can be obtained using the engine test bench. Moreover, φ_{cool} is the heat transfer efficiency of the Evaporator 2 and T_{HTL} is the temperature of the high temperature heat source in the LT loop ORC system. This temperature is assumed to be equal to $T_{HTL} = T_{L1} + 5$.

Expander phase (stages L1–L2):

The power output of the expander 2 and its exergy destruction rate are respectively calculated using the following equations:

$$\dot{W}_{exp2} = \dot{m}_L(h_{L1} - h_{L2}) \tag{22}$$

$$\dot{I}_{exp2} = T_0\dot{m}_L(s_{L2} - s_{L1}) \tag{23}$$

The isentropic efficiency of the Expander 2 is given by:

$$\eta_{exp2} = \frac{h_{L1} - h_{L2}}{h_{L1} - h_{L2s}} \tag{24}$$

Condenser phase (stages L2–L3):

The heat transfer rate of the condenser and its exergy destruction rate are respectively calculated using the following:

$$\dot{Q}_{con} = \dot{m}_L(h_{L2} - h_{L3}) \tag{25}$$

$$\dot{I}_{con} = T_0\dot{m}_L\left[(s_{L3} - s_{L2}) - \frac{h_{L3} - h_{L2}}{T_{LTL}}\right] \tag{26}$$

where T_{LTL} is the temperature of the low temperature heat source in the LT loop ORC system. This temperature is assumed to be equal to $T_{LTL} = T_{L3} - 5$.

2.3. Performance parameters of the dual loop ORC system

To evaluate the performance of the dual loop ORC system, the following parameters are selected for the study:

The net power output of the HT loop ORC system is calculated as:

$$\dot{W}_{H,n} = \dot{W}_{exp1} - \dot{W}_{p1} \tag{27}$$

The exergy destruction rate of the HT loop ORC system is calculated as:

$$\dot{I}_H = \dot{I}_{p1} + \dot{I}_r + \dot{I}_{e1} + \dot{I}_{exp1} \tag{28}$$

The net power output of the LT loop ORC system is calculated as:

$$\dot{W}_{L,n} = \dot{W}_{exp2} - \dot{W}_{p2} \tag{29}$$

The exergy destruction rate of the LT loop ORC system is calculated as:

$$\dot{I}_L = \dot{I}_{p2} + \dot{I}_{int} + \dot{I}_{pre} + \dot{I}_{e2} + \dot{I}_{exp2} + \dot{I}_{con} \tag{30}$$

The overall net power output of the dual loop ORC system is defined as:

$$\dot{W}_{oa,n} = \dot{W}_{H,n} + \dot{W}_{L,n} \tag{31}$$

The waste heat recovery efficiency (WHRE) of the dual loop ORC system is calculated as:

$$\eta_w = \frac{\dot{W}_{oa,n}}{\dot{Q}_w} \tag{32}$$

where $\dot{Q}_w$ is the overall waste heat generated by the diesel engine, which is calculated as:

$$\dot{Q}_w = \dot{Q}_{exh} + \dot{Q}_{int} + \dot{Q}_{cool} \tag{33}$$

where $\dot{Q}_{exh}$ is the exhaust energy of the diesel engine.

In this study, assumptions about the restricted conditions for the dual loop ORC system are listed as follows:

(1) The system operates under steady condition, there are no pressure drops in pipes and heat exchangers; heat losses in each component are also neglected.
(2) In the HT loop ORC system, the evaporation pressure is set to 3 MPa, and the condensation temperature is set to 353.15 K.
(3) The isentropic efficiencies of Expanders 1 and 2 are both set to 0.7. The isentropic efficiencies of Pumps 1 and 2 are both set to 0.65. The effectiveness of the recuperator is set to 0.85, and the heat transfer efficiency of the preheater is set to 0.85.
(4) The ambient temperature is set to 291.15 K.
(5) As the coolant temperature of the diesel engine is often maintained at 363.15 K, to ensure a reasonable heat transfer temperature difference between the engine coolant and the working fluid, the evaporation temperature is set to 348.15 K in the LT loop ORC system. The condensation temperature is set to 293.15 K.

(6) In the working process of the coolant system, a large proportion of the heat dissipates into the air. Only a small part of the heat can be utilized [19,20]. Thus, in the calculation process, the heat transfer efficiency of the Evaporator 2 is set to 0.3.

3. Characteristic analysis of the diesel engine waste heat

To design a reasonable ORC system to utilize various waste heats from the diesel engine with high efficiency, studying the energy distribution in the running process of the diesel engine is necessary. A six-cylinder in-line diesel engine is used as the object of analysis. The main technical performance parameters are listed in Table 2.

In Fig. 3, the performance map of the diesel engine is plotted based on the test results from the diesel engine test bench. Therein, the blue contour lines indicate the variations in the effective power output of the diesel engine with the engine speed and engine torque. The black contour lines indicate the variations in the brake specific fuel consumption (BSFC) of the diesel engine with the engine speed and engine torque. According to the measured test data, the engine speed varies in the range of about 900 r/min to 1900 r/min, and the engine torque varies in the range of about 100 N m to 1500 N m. At the engine rated condition, the effective power output of the diesel engine is 247 kW. When the engine is running in the working region where the engine speed varies in the range of 1400 r/min to 1700 r/min and the engine torque varies in the range of 1200 N m to 1500 N m, the diesel engine achieves the optimal fuel economy, and the BSFC is 194 g/(kW.h). The diesel engine generally operates at a high speed and with a high load. Therefore, this diesel engine has good fuel economy.

Fig. 4 shows the exhaust temperature and exhaust mass flow rate of the diesel engine measured from the test. Fig. 4a shows that when the diesel engine is running with a medium–low load, the diesel engine exhaust temperature is affected less by the engine speed and increases primarily with the engine load. When the engine is operating with medium–low speed and medium–high load, the diesel engine exhaust temperature is relatively high and can reach 667 K. As shown in Fig. 4b, the exhaust mass flow rate of the diesel engine increases with the engine speed and engine load. This change primarily depends on the fuel consumption and the intake air mass flow rate. The intake air mass flow rate varies primarily with the engine speed whereas the engine load mainly affects fuel consumption. At the engine rated condition, the exhaust mass flow rate can reach up to 0.36 kg/s.

The distribution of fuel energy released by combustion under a certain operating condition of the diesel engine is depicted using the first law of thermodynamics, which is:

$$\dot{Q}_{comb} = \dot{m}_f h_f + \dot{m}_a h_a = \dot{W}_{eff} + \dot{Q}_{exh} + \dot{Q}_{cool} + \dot{Q}_{misc} \quad (34)$$

where $\dot{Q}_{comb}$ is the fuel energy released by combustion when the engine is running, $\dot{m}_f$ and $\dot{m}_a$ are the fuel and air mass flow rates, respectively. h_f and h_a are the corresponding inlet enthalpies. $\dot{W}_{eff}$ is the effective power output of the diesel engine and can be measured with the diesel engine test bench. Exhaust energy $\dot{Q}_{exh}$ is calculated using an approximation method. $C_xH_yO_z$ can denote the average molecular composition for common diesel fuel because the petroleum-derived diesel fuel composition is very complicated. In this composition, x, y, and z respectively represent the moles of the C, H, O. Based on the atomicity balance principle, the overall complete combustion equation is:

$$C_xH_yO_z + \left(x + \frac{y}{4} - \frac{z}{2}\right)(O_2 + 3.773N_2) = xCO_2 + \frac{y}{2}H_2O + 3.773\left(x + \frac{y}{4} - \frac{z}{2}\right)N_2 \quad (35)$$

The air–fuel ratio is controlled using a stoichiometric ratio to maintain the high efficiency of the three-way catalytic converter. The mass fraction of the exhaust compositions CO_2, H_2O and N_2 can then be calculated using Eq. (35). Generally, the exhaust temperature is above 500 K, and the exhaust pressure is slightly higher than atmospheric pressure. Thus, the specific enthalpy of the exhaust gas can be calculated using a calculation method for mixture gas [30].

$$h_{exh}(T,P) = \chi_{CO_2} h_{CO_2}(T,P) + \chi_{H_2O} h_{H_2O}(T,P) + \chi_{N_2} h_{N_2}(T,P) \quad (36)$$

$$\dot{Q}_{exh} = \dot{m}_{exh} h_{exh} \quad (37)$$

Finally, exhaust energy can be computed using Eq. (37). In addition, $\dot{Q}_{misc}$ is the heat rejected to the oil plus convection and radiation from engine's external surface. As the miscellaneous heat loss normally accounts for 3% to 10% of the overall combustion energy of a diesel engine, a fixed value 9% was used in this study [31]. Finally, the exhaust energy and the heat transfer rate to the coolant are evaluated at each operating condition over the whole operating range by using the Eqs. (34)–(37).

Fig. 5 shows the variation of each type of energy in the diesel engine, which were calculated using the above-mentioned equations under engine various operating conditions. The fuel energy released by combustion is shown in Fig. 5a. As the engine speed and engine load increases, the fuel energy released by combustion increases gradually. Such phenomenon is primarily caused by the increase in fuel consumption and intake air mass. At the engine rated condition, the fuel energy released by combustion reaches the upper limit and is approximately 787 kW. Figs. 5b and c show that, the variation tendencies of the engine effective power output and the exhaust energy of the diesel engine, over the whole oper-

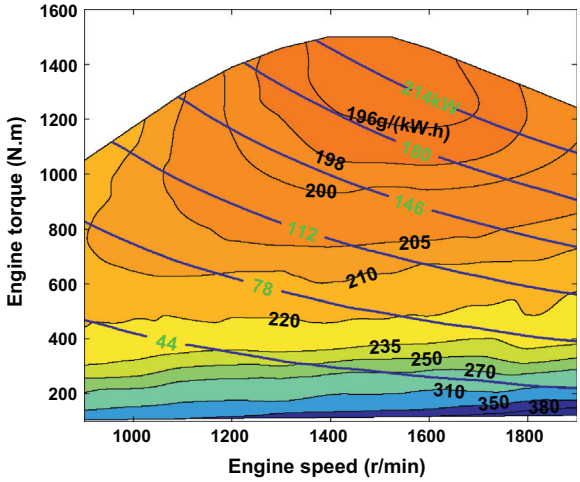

Fig. 3. Performance map of the diesel engine.

Table 2
The main technical performance parameters of the diesel engine.

Items	Parameters	Units
Rated power	247	kW
Maximum torque	1600	N m
Displacement	11.596	L
Cylinder number	6	
Air intake type	Turbocharged and Intercooled	
Fuel injection system	High pressure common rail	
Speed at maximum torque	1400	r/min
Stroke and cylinder bore	155 × 126	mm
Compression ratio	17.1	

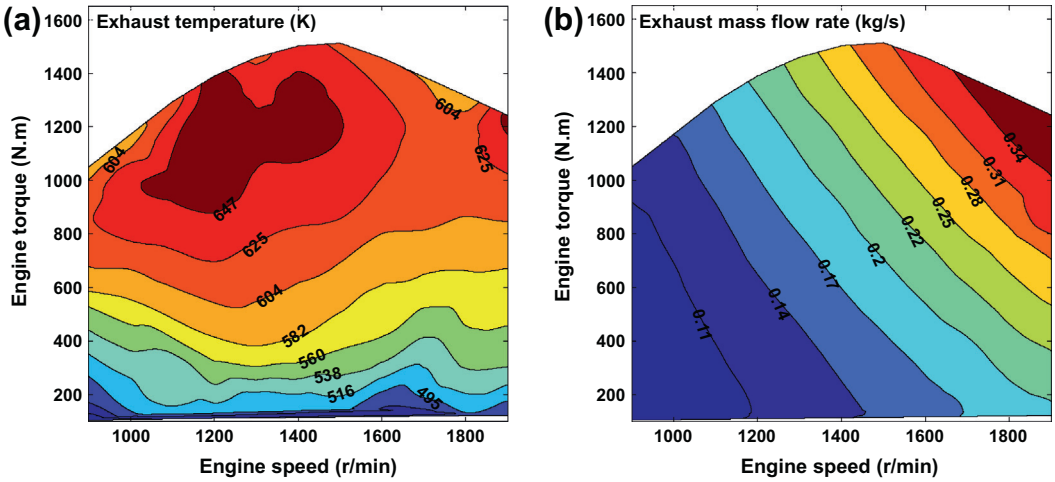

Fig. 4. Variation of exhaust temperature and exhaust mass flow rate of the diesel engine.

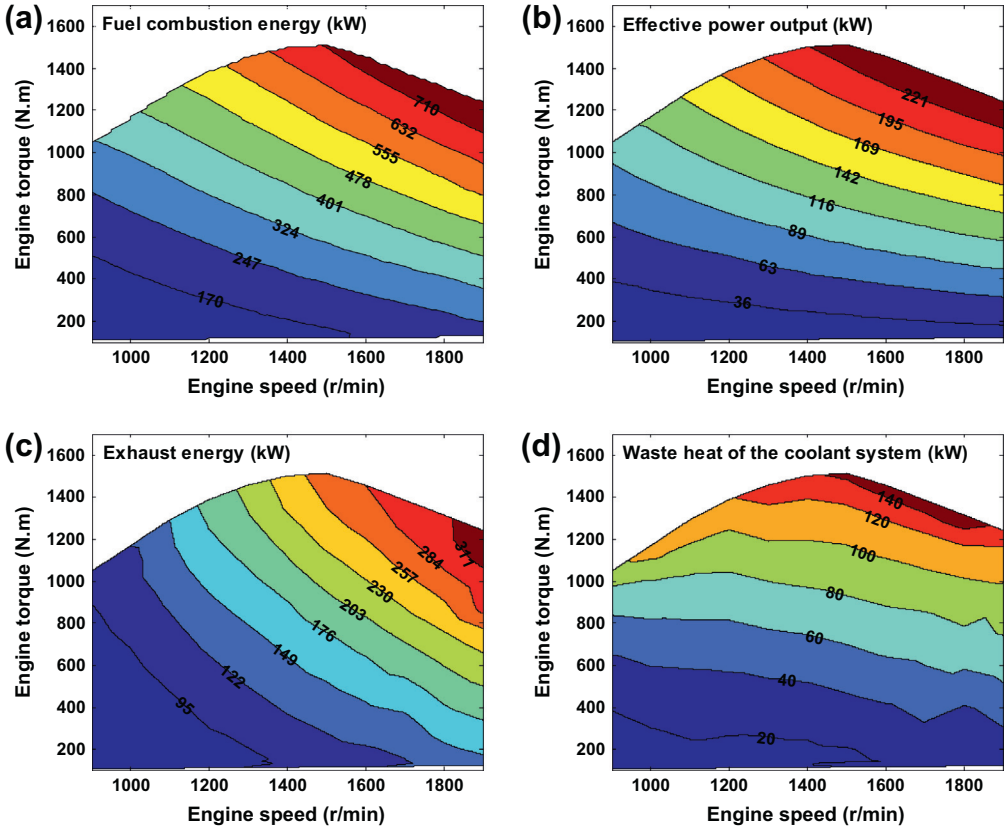

Fig. 5. Energy distribution of the diesel engine.

ating range, are basically in accordance with that of the overall energy generated from the fuel combustion. Thus, all increase with the engine speed and engine load. At the engine rated condition, the exhaust energy reaches the upper limit and is approximately 338 kW. Over the whole operating range, the variation of the waste heat quantity carried by the coolant system is shown in Fig. 5d. The engine load primarily affects the waste heat quantity carried by the coolant system. When the engine is operating at medium–high speed and high load, the coolant system obtains the maximum waste heat quantity and is about 158 kW. The comparison of different energies, over the whole operating range, is shown in Fig. 6. It can be concluded that, of the overall energy generated from the fuel combustion, only a relatively small proportion is used to produce useful work output, a large proportion of the energy is wasted, and the fuel energy released by combustion is far more than the effective power output of the diesel engine. Fig. 6 shows that, over the whole operating range, the exhaust energy is greater than the engine effective power output. Meanwhile, part of the waste heat within the coolant system can be recovered. Therefore, recovering and utilizing the waste heat of the diesel engine is very important.

Fig. 7 shows the variations in the main performance parameters of the intercooler, which were measured using the diesel engine test bench. The intake air temperature and pressure at the inlet

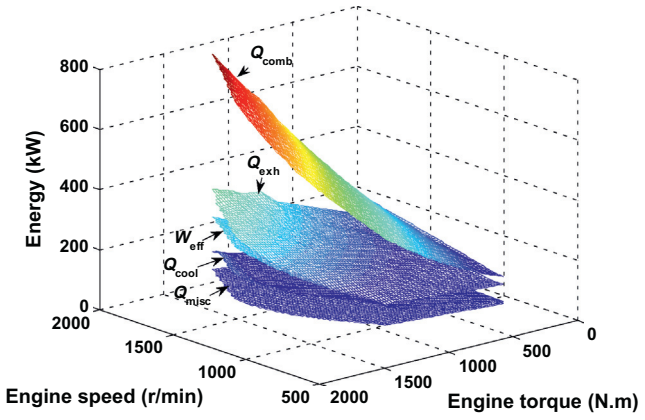

Fig. 6. Energy comparison of the diesel engine.

of the intercooler are depicted in Fig. 7a and b respectively. With the increase of the engine speed and engine load, the intake air temperature and pressure increase gradually. The intake air temperature at the inlet of the intercooler varies in the range of 309 K to 407 K, and can be used to heat the subcooled liquid working fluid in the LT loop ORC system. At the engine rated condition, the intake air temperature at the inlet of the intercooler can reach 407 K, the intake air pressure at the inlet of the intercooler can reach 2.44 bar. The intake air temperature at the outlet of the intercooler is shown in Fig. 7c. When the engine is running at low speed, the intake air temperature at the outlet of the intercooler is barely affected by the engine load. The intake air temperature at the outlet of the intercooler greatly affects engine performance. Thus, regulating the intake air temperature at the outlet of the intercooler is necessary. Fig. 7d shows the variation of the released heat from the turbocharged air in the intercooler over the whole operating range. The released heat from turbocharged air in the intercooler increases with the engine speed and engine load. At the engine rated condition, the released heat from turbocharged air in the intercooler reaches the upper limit and is 40.65 kW.

4. Results and discussion

According to the study above on the characteristics of waste heat distribution over the whole operating range and based on the established thermodynamic model of the dual loop ORC system, the potential of the dual loop ORC system for waste heat recovery over the whole operating range is analyzed. The mass flow rate of the working fluid and net power output in the HT loop ORC system are shown in Fig. 8. The mass flow rate of the working fluid and net power output in the HT loop ORC system have the same variation tendency. All increase with the engine speed and engine load. At the engine rated condition, the mass flow rate of the working fluid is 0.66 kg/s, and the net power output is 10 kW. Eqs. 1, 9, and 27 show that, the net power output of the ORC system depends on the mass flow rate of the working fluid. Note that the variation tendencies of the working fluid and the net power output in Fig. 8 are very similar to that of the exhaust energy in Fig. 5c because the mass flow rate and net power output are proportional to the heat transferred inside of Evaporator 1. More exhaust energy, results in a larger mass flow rate of the working fluid, and a larger net power output of the HT loop ORC system. Through the comparison between Fig. 5c and Fig. 8, it can be concluded that the mass flow rate of the working fluid and net power output have the same variation tendency with the exhaust energy of the diesel engine.

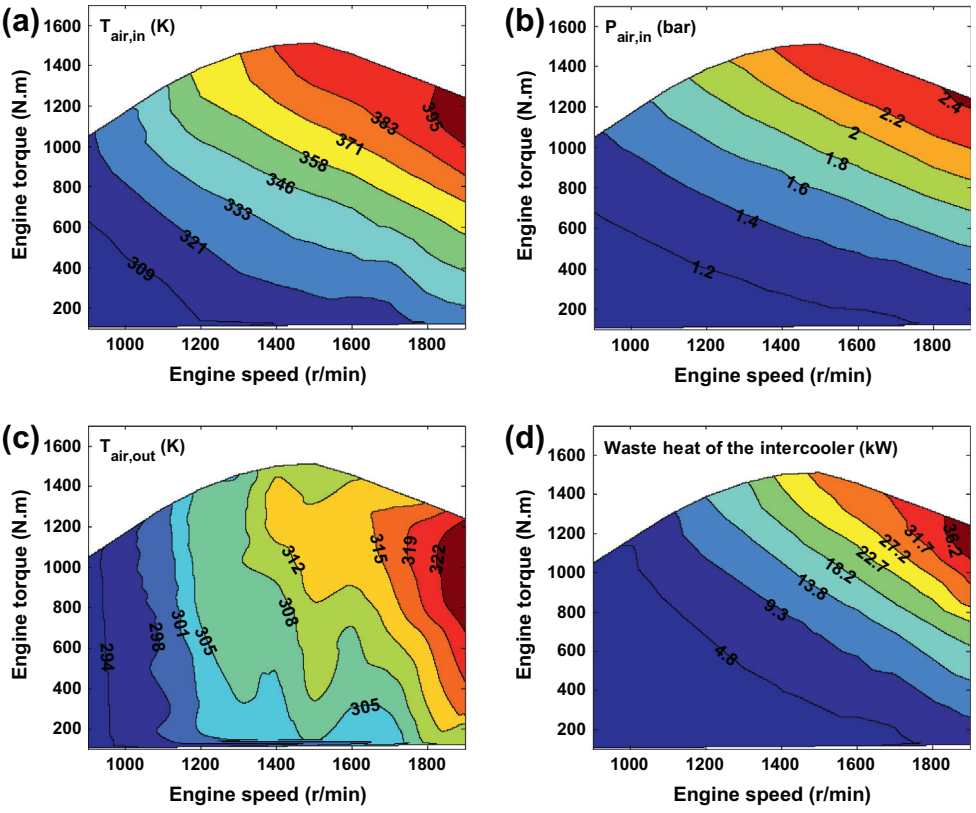

Fig. 7. Performance parameters of the intercooler.

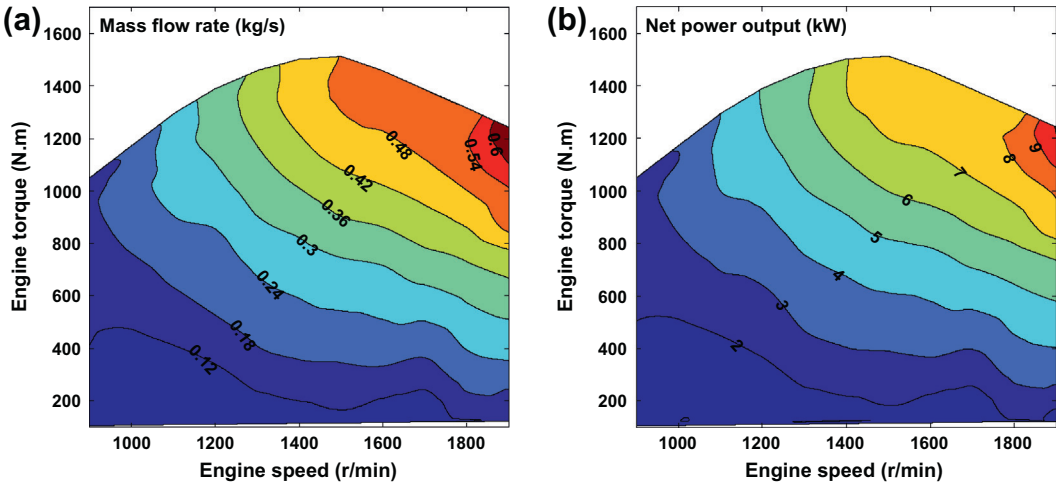

Fig. 8. Mass flow rate of the working fluid and net power output in the HT loop ORC system.

Fig. 9 shows the mass flow rate of the working fluid and net power output in the LT loop ORC system over the whole operating range. Likewise, similar to the HT loop ORC system, the mass flow rate of the working fluid and net power output increase with the engine speed and engine load. At the engine rated condition, the net power output of the LT loop ORC system reaches the upper limit and is 17.85 kW. The comparison between Figs. 8 and 9 show that for the majority of the engine operating conditions, the mass flow rate of the working fluid and net power output in the LT loop ORC system are all greater than that of the HT loop ORC system. This characteristic is particularly evident when the engine is operating at a high speed with a high load region. Over the whole operating range, the heat absorbed by the HT loop ORC system is contrasted with that by the LT loop ORC system in Fig. 10. The heat absorbed by the LT loop ORC system is obviously higher than the heat absorbed by the HT loop ORC system because the heat absorbed by the LT loop ORC system contains the waste heat from the coolant system, the released heat from turbocharged air in the intercooler, and the released heat in condensation process of the HT loop ORC system. Though the waste heat utilized by the LT loop ORC system is usually at a lower temperature in contrast with the HT loop, the waste heat quantity is greater and worth recovering.

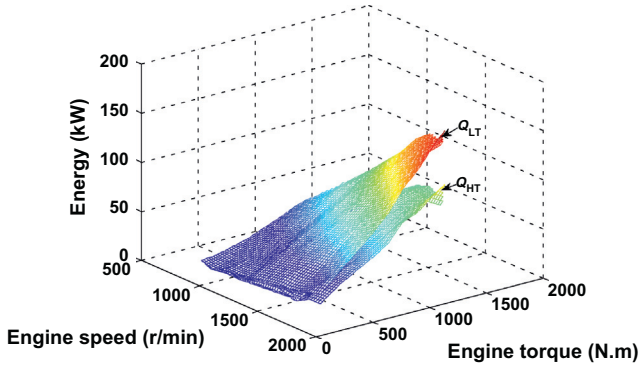

Fig. 10. Comparison of the absorbed heat between the HT loop ORC system and LT loop ORC system.

Fig. 11 shows the variation of the overall net power output of the dual loop ORC system over the whole operating range. The overall net power output is the sum of the net power output of the HT loop ORC system and the net power output of the LT loop ORC system. In terms of the analysis results mentioned above, the net power outputs of both the HT and LT loop ORC system in-

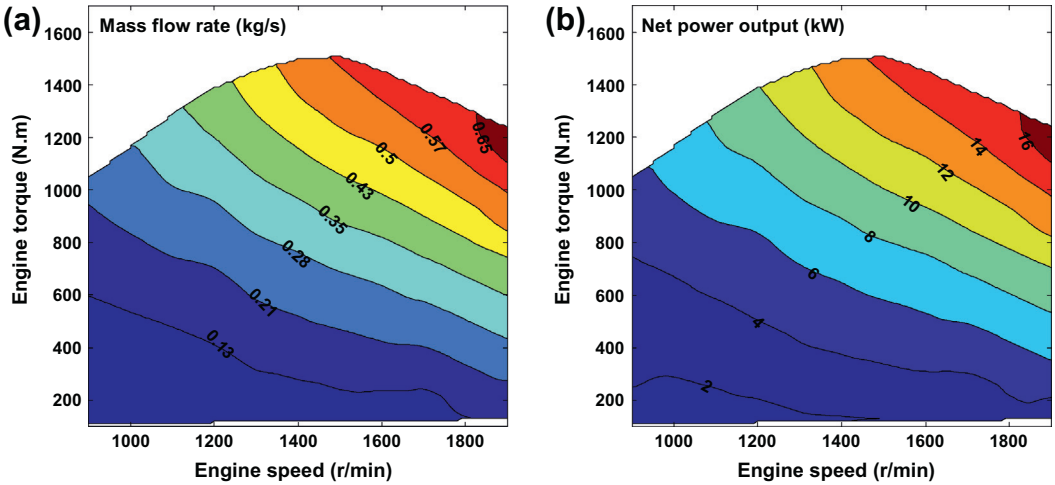

Fig. 9. Mass flow rate of working fluid and net power output in the LT loop ORC system.

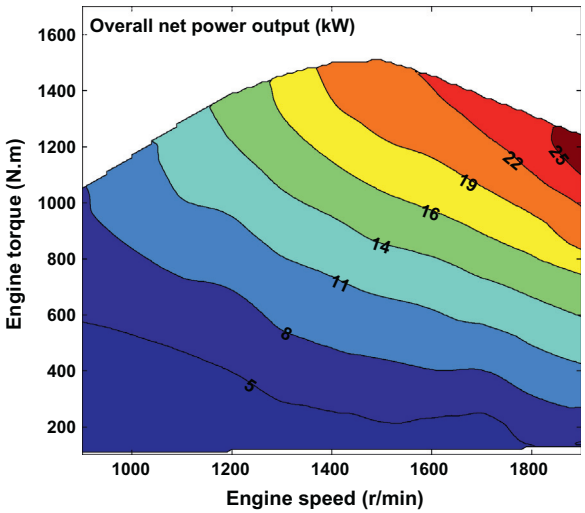

Fig. 11. Overall net power output of the dual loop ORC system.

crease with the engine speed and engine load. Therefore, the overall net power output of the dual loop ORC system has the same variation tendency. At the engine rated condition, the overall net power output of the dual loop ORC system reaches the upper limit and is 27.85 kW.

The WHRE of the dual loop ORC system is given in Fig. 12. When the engine operates at a high load region, the maximum value is 5.4%. The comparison between Figs. 4a and 12 show that WHRE and exhaust temperature have the same variation tendency, and both are primarily affected by the engine load. Figs. 5 and 6 show that when the engine operates with medium–high speed and medium–high load, the exhaust energy, waste heat quantity carried by the engine coolant system, and released heat from the turbocharged air in the intercooler are far greater than that of other working conditions. The waste heat absorbed by the dual loop ORC system also increases apparently. Thus, the dual loop ORC system that possesses higher WHRE is proven to be more suitable for the medium–high engine load.

To assess the fuel economy of the diesel engine-dual loop ORC combined system, the effective thermal efficiency of the combined system is defined as:

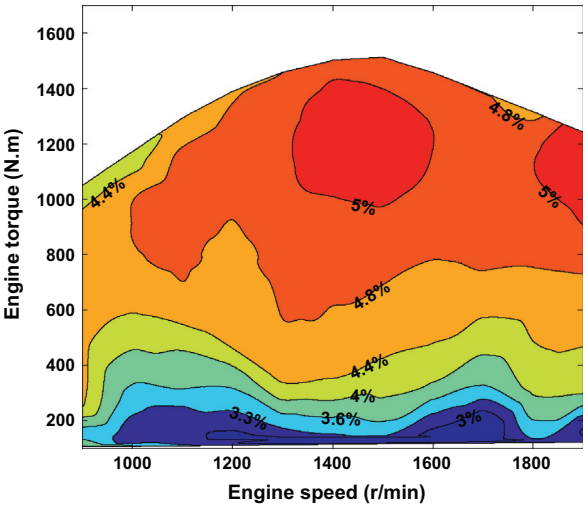

Fig. 12. WHRE of the dual loop ORC system.

$$\eta_{th,cs} = \frac{\dot{W}_{eff} + \dot{W}_{oa,n}}{\dot{Q}_{comb}} \tag{38}$$

The BSFC of the combined system is defined as follows:

$$bsfc_{cs} = \frac{\dot{F}}{\dot{W}_{eff} + \dot{W}_{oa,n}} \times 1000 \tag{39}$$

where $\dot{F}$ represents the fuel consumption of the diesel engine.

Fig. 13 shows the comparison of the effective thermal efficiency between the diesel engine and the combined system over the whole operating range. The figure shows that after the dual loop ORC system is combined with the diesel engine, the effective thermal efficiencies of the combined system over the whole operating range are all higher than that of the diesel engine itself. Morever, the effective thermal efficiency of the combined system has the same variation tendency with that of the diesel engine itself. In addition, when the engine operates with a medium–high load, both the diesel engine and the combined system have relatively high effective thermal efficiencies, and all are barely affected by the engine speed. Thus, the diesel engine that generally runs with a high load has relatively high energy utilization efficiency. At the engine rated conditon, the effective thermal efficiency of the combined system is 0.35, which increases by 13% compared with the diesel engine itself.

Fig. 14 shows the variations of the BSFC of the diesel engine-dual loop ORC combined system. Compared with Fig. 3, all the BSFCs of the combined system can be concluded to an improvement compared with the diesel engine itself over the whole operating range. When the engine operates in the medium–high load region, the fuel economy of the combined system is better, and the BSFC can decrease to 186 g/(kW h). Compared with the diesel engine itself, the BSFC can be reduced by 4%. Therefore, the fuel economy of the diesel engine combined with the dual loop ORC system is effectively improved.

The performance of the dual loop ORC system is not only affected by the mass flow rate of the working fluid, but also by the thermodynamic parameters of the working fluids at each state point of the system, such as pressure, temperature, enthalpy, and entropy. At the engine rated condition, the results for the thermodynamic properties of the working fluids are given in Table 3. With these results, the operating states of the system can be determined. In the HT loop and LT loop ORC systems, variation in the exergy destruction rate of each component over the whole operating range are shown in Figs. 15 and 16, respectively. In the HT loop ORC system, Evaporator 1 and Expander 1 have a higher exergy destruction rate, and both increase with the engine speed and load. In this paper, the operating parameters of the system were given, and the temperatures of high temperature heat source and low temperature heat source are all assumed to be constant values.

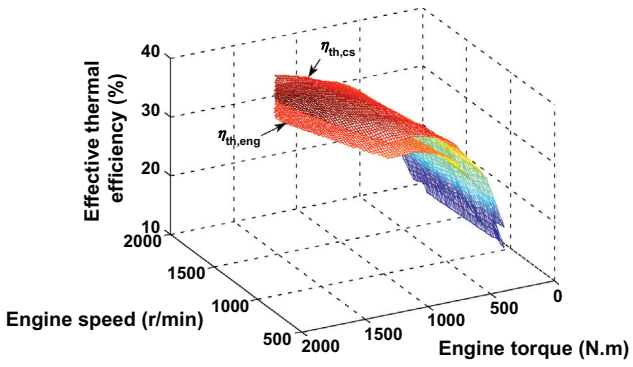

Fig. 13. Comparison of the effective thermal efficiency.

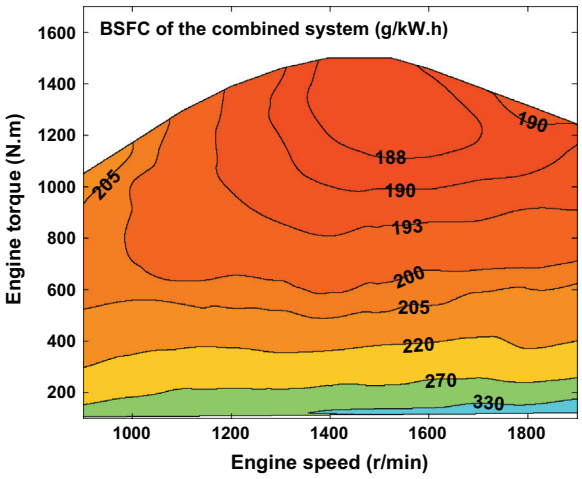

Fig. 14. BSFC of the combined system.

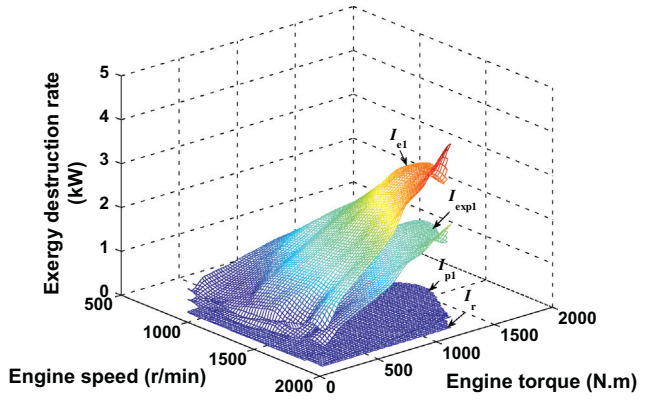

Fig. 15. Comparison of the exergy destruction rate of each component in the HT loop ORC system.

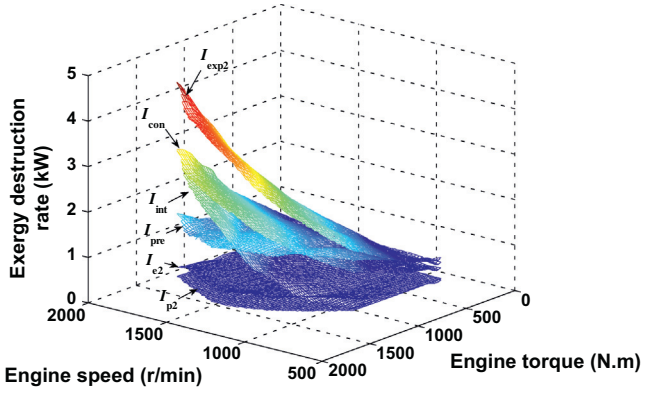

Fig. 16. Comparison of the exergy destruction rate of each component in the LT loop ORC system.

Thus, according to Eqs. (8) and (10), exergy destruction rates of Evaporator 1 and Expander 1 have the same variation tendency with the mass flow rate of the working fluid. That is, both increase with engine speed and load. At the engine rated condition, the exergy destruction rates of Evaporator 1 and Expander 1 all reach the upper limit, which are 4.21 kW and 2.36 kW, respectively. Moreover, the exergy destruction rates of the recuperator and Pump1 are all relatively low, and the variation of the exergy destruction rate is very small under various operating conditions. These findings are because their entropy differences between the inlet and outlet working fluids are very small as seen from the calculating results. In the LT loop ORC system, exergy destruction rates of Expander 2, the condenser, and the intercooler are all relatively high and increase dramatically with engine speed and load. At the engine rated condition, the exergy destruction rates of Expander 2, the condenser and the intercooler all reach the upper limit and are 4.35 kW, 2.04 kW and 2.06 kW, respectively. Fig. 16 shows that, with the varying operating conditions, the exergy destruction rate of the preheater varies slightly. At the engine rated condition, its exergy destruction rate reaches the upper limit, which is 1.45 kW. The exergy destruction rates of the Evaporator 2 and Pump 2 are relatively low, and are only 0.28 kW and 0.07 kW, respectively. The aforementioned analysis shows that, reducing the exergy destruction rate of the expander and the heat exchanger is necessary for lowering the irreversibility of the dual loop ORC system.

Over the whole operating range, the variations in the exergy destruction rates of the LT loop ORC system, HT loop ORC system, and the dual loop ORC system are shown in Fig. 17. The overall exergy destruction rate of the dual loop ORC system is the sum of the exergy destruction rate of each component of the both LT and HT loop ORC system. The increase of the engine speed and load causes the exergy destruction rate of HT loop ORC system and LT loop ORC system to increase gradually, and the exergy destruction rate of the LT loop is higher than that of the HT loop. Figs. 4a and 7a show that when the engine is running with high speed and high load, the exhaust temperature and the intake air temperature at the inlet of the intercooler increase markedly. Therefore, the temperature difference between the heat source and the working fluid

Table 3
Thermodynamic properties of the working fluids at the engine rated condition.

State point	Pressure (MPa)	Temperature (K)	Enthalpy (kJ/kg)	Entropy (kJ/kg K)
HT loop ORC				
H1	3	416.35	487.93	1.791
H2	0.789	360.47	470.43	1.804
H3	0.789	355.68	464.78	1.788
H4	0.789	353.15	309.24	1.347
H5	3	354.84	311.59	1.349
H6	3	358.68	317.24	1.365
LT loop ORC				
L1	0.695	348.15	458.40	1.776
L2	0.122	308.22	433.21	1.797
L3	0.122	293.15	225.86	1.091
L4	0.695	293.41	226.39	1.091
L5	0.695	334.72	282.53	1.270
L6	0.695	348.15	425.22	1.681

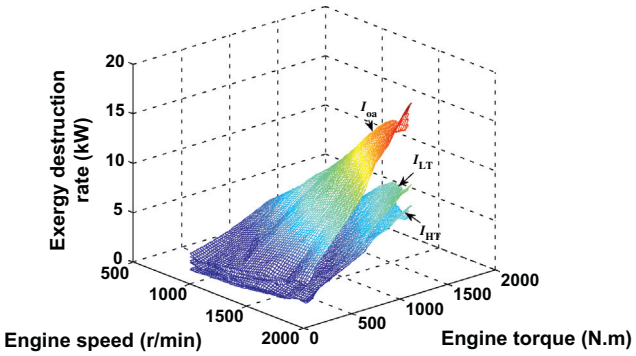

Fig. 17. Comparison of the exergy destruction rate.

is larger, thus resulting in the greater irreversibility of the heat exchanger. In addition, with the increase in engine waste heat, the mass flow rate of dual loop ORC system increases and leads the increase in the exergy destruction rate of each component in the system. At the engine rated condition, the exergy destruction rates of HT loop and LT loop, which are 8.29 kW and 10.42 kW respectively, hit the top. Compared with the HT loop, the amount of components that comprise the LT loop ORC system is greater, and the mass flow rate of the working fluid is larger. Therefore, the exergy destruction rate of the LT loop is higher than that of the HT loop. Though, after bring equipped with LT loop ORC system, the exergy destruction rate of the dual loop ORC system can be increased dramatically. However, the cascade utilization of engine waste heat can be realized, and then the net power output of the dual loop ORC system can be effectively increased thereby. It also can be observed from Fig. 17 that, at the engine rated condition, the overall exergy destruction rate of the dual loop ORC system hits the top and is 18.71 kW.

5. Conclusions

In this paper, in order to realize the cascade utilization of diesel engine waste heat, a set of dual loop ORC system is designed, with R245fa is chosen as the working fluid, to recover exhaust energy, waste heat from the coolant system, and released heat from turbocharged air in the intercooler. Based on an analysis of the distribution characteristics of the diesel engine waste heat and the operating performance of the diesel engine-dual loop ORC combined system, conclusions can be made as follows:

(1) By employing the dual loop ORC system, the fuel economy of the diesel engine can be notably improved. At the engine rated condition, the effective thermal efficiency of the diesel engine-dual loop ORC combined system is 0.35, which increases by 13% compared with the diesel engine itself. When the engine is operating in medium–high load region, the combined system has better fuel economy, the BSFC can be decreasd to 186 g/(kW h) and can be improved by a maximum of 4% compared with the diesel engine itself.

(2) For most operating conditions of the diesel engine, the net power output of the LT loop ORC system is greater than that of the HT loop ORC system. At the engine rated condition, the net power output of the LT loop ORC system is 17.85 kW, the net power output of the HT loop ORC system is 10 kW, the overall net power output of the dual loop ORC system is 27.85 kW. Over the whole operating range, the WHRE of the combined system can reach a maximum of 5.4%.

(3) For the dual loop ORC system, over the whole operating range, the overall exergy destruction rate of the dual loop ORC system increases with the engine speed and engine load, such that the exergy destruction rate of the LT loop ORC system is higher than that of the HT loop ORC system. At the engine rated condition, the exergy destruction rate of the LT loop ORC system is 10.42 kW, whereas exergy destruction rate of the HT loop ORC system is 8.29 kW.

Acknowledgments

This work was sponsored by the National Natural Science Foundation of China (Grant No. 51376011), Beijing Natural Science Foundation Program and Scientific Research Key Program of Beijing Municipal Commission of Education (Grant No. KZ201410005003), the National Basic Research Program of China (973 Program) (Grant No. 2011CB707202), the Tenth Scientific Research Foundation for Graduate Students in North University of China (Grant No. 20131006) and the Twelfth Scientific Research Foundation for Graduate Students in Beijing University of Techonlogy (Grant No. ykj–2013–9302).

References

[1] Ma FR, Hanna MA. Biodiesel production: a review[1]. Bioresour Technol 1999;70:1–15.
[2] Chisti Y. Biodiesel from microalgae. Biotechnol Adv 2007;25:294–306.
[3] Dehkordi AM, Ghaseni M. Transesterification of waste cooking oil to biodiesel using Ca and Zr mixed oxides as heterogeneous base catalysts. Fuel Process Technol 2012;97:45–51.
[4] Mago PJ, Chamra LM, Srinivasan K, Somayaji C. An examination of regenerative organic Rankine cycles using dry fluids. Appl Therm Eng 2008;28:998–1007.
[5] Wang ZQ, Zhou NJ, Guo J, Wang XY. Fluid selection and parametric optimization of organic Rankine cycle using low temperature waste heat. Energy 2012;40:107–15.
[6] Roy JP, Mishra MK, Misra A. Parametric optimization and performance analysis of a waste heat recovery system using Organic Rankine Cycle. Energy 2010;35:5049–62.
[7] Wei DH, Lu XS, Lu Z, Gu JM. Performance analysis and optimization of organic Rankine cycle (ORC) for waste heat recovery. Energy Convers Manage 2007;48:1113–9.
[8] Liu B, Rivière P, Coquelet C, Gicquel R, David F. Investigation of a two stage Rankine cycle for electric power plants. Appl Energy 2012;100:285–94.
[9] Wang JF, Yan ZQ, Wang M, Li MQ, Dai YP. Multi-objective optimization of an organic Rankine cycle (ORC) for low grade waste heat recovery using evolutionary algorithm. Energy Convers Manage 2013;71:146–58.
[10] Gao H, Liu C, He C, Xu XX, Wu SY, Li YR. Performance analysis and working fluid selection of a supercritical organic Rankine cycle for low grade waste heat recovery. Energies 2012;5:3233–47.
[11] Hung TC. Waste heat recovery of organic Rankine cycle using dry fluids. Energy Convers Manage 2001;42:539–53.
[12] Quoilin S, Aumann R, Grill A, Schuster A, Lemort V, Spliethoff H. Dynamic modeling and optimal control strategy of waste heat recovery Organic Rankine cycles. Appl Energy 2011;88:2183–90.
[13] Dai YP, Wang JF, Gao L. Parametric optimization and comparative study of organic Rankine cycle (ORC) for low grade waste heat recovery. Energy Convers Manage 2009;50:576–82.
[14] Guo T, Wang HX, Zhang SJ. Selection of working fluids for a novel low-temperature geothermally-powered ORC based cogeneration system. Energy Convers Manage 2011;52:2384–91.
[15] Hung TC, Wang SK, Kuo CH, Pei BS, Tsai KF. A study of organic working fluids on system efficiency of an ORC using low-grade energy sources. Energy 2010;35:1403–11.
[16] Wang XD, Zhao L, Wang JL. Experimental investigation on the low-temperature solar Rankine cycle system using R245fa. Energy Convers Manage 2011;52:946–52.
[17] Gao WZ, Zhai JM, Li GH, Bian Q, Feng LM. Performance evaluation and experiment system for waste heat recovery of diesel engine. Energy 2013;55:226–35.
[18] Srinivasan KK, Mago PJ, Krishnan SR. Analysis of exhaust waste heat recovery from a dual fuel low temperature combustion engine using an Organic Rankine cycle. Energy 2010;35:2387–99.
[19] Vaja I, Gambarotta A. Internal combustion engine (ICE) bottoming with Organic Rankine cycle (ORCs). Energy 2010;35:1084–93.
[20] Yu GP, Shu GQ, Tian H, Wei HQ, Liu LN. Simulation and thermodynamic analysis of a bottoming Organic Rankine cycle (ORC) of diesel engine (DE). Energy 2013;51:281–90.

[21] Tian H, Shu GQ, Wei HQ, Liang XY, Liu LN. Fluids and parameters optimization for the organic Rankine cycles (ORCs) used in exhaust heat recovery of Internal Combustion Engine (ICE). Energy 2012;47:125–36.
[22] Katsanos CO, Hountalas DT, Pariotis EG. Thermodynamic analysis of a Rankine cycle applied on a diesel truck engine using steam and organic medium. Energy Convers Manage 2012;60:68–76.
[23] Wang EH, Zhang HG, Zhao Y, Fan BY, Wu YT, Mu QH. Performance analysis of a novel system combining a dual loop organic Rankine cycle (ORC) with a gasoline engine. Energy 2012;43:385–95.
[24] Peng ZJ, Wang TY, He YL, Yang XY, Lu LP. Analysis of environmental and economic benefits of integrated Exhaust Energy Recovery (EER) for vehicles. Appl Energy 2013;105:238–43.
[25] Wang TY, Zhang YJ, Zhang J, Shu GQ, Peng ZJ. Analysis of recoverable exhaust energy from a light-duty gasoline engine. Appl Therm Eng 2013;53:414–9.
[26] Wang EH, Zhang HG, Fan BY, Ouyang MG, Zhao Y, Mu QH. Study of working fluid selection of organic Rankine cycle (ORC) for engine waste heat recovery. Energy 2011;36:3406–18.
[27] REFPROP version 8.0. NIST standard reference database 23. The US Secretary of commerce, America; 2007.
[28] Bahadori A. Estimation of combustion flue gas acid dew point during heat recovery and efficiency gain. Appl Therm Eng 2011;31:1457–62.
[29] Roy JP, Mishra MK, Mishra A. Performance analysis of an Organic Rankine cycle with superheating under different heat source temperature conditions. Appl Energy 2011;88:2995–3004.
[30] Poling BE, Prausnitz JM, O' Connell JP. The properties of gases and liquids. 6th ed. New York: McGraw-Hill; 2001.
[31] Heywood JB. Internal combustion engine fundamentals. New York: McGraw-Hill; 1988.